Check for updates

Published online June 28, 2005

Reproduced from Soil Science Society of America Journal. Published by Soil Science Society of America. All copyrights reserved.

Modeling Energy Inputs to Predict Pedogenic Environments Using Regional Environmental Databases

Craig Rasmussen,* Randal J. Southard, and William R. Horwath

ABSTRACT

We present a model for prediction of pedogenic environments and soil properties based on energy input to the soil system. The model estimates rates of precipitation and net primary production (NPP) energy input using the Parameter-Regression Independent Slope Model (PRISM) climate data, and a parent material index (PMI). Soil order, soil C, and clay data from the State Soil Geographic (STATSGO) database were compared with rates of NPP and precipitation energy input for major geographic regions of the continental USA, including California, Oregon, Washington, Texas, North Dakota, Alabama, Pennsylvania, and New Hampshire. Soil orders in all states show differences in total energy input (E_{in}, kJ $m^{-2}yr^{-1}$) and the percentage of E_{in} from NPP (%E_{npp}) (e.g., Ultisols E_{in} = 29 915, %E_{npp} = 49%; Mollisols E_{in} = 5880, %E_{npp} = 90%). Using linear regression models, rates of NPP estimated (R^2 = 0.82*) trends in soil C content in western states, but failed to estimate soil C in other geographic areas. Parent material index adjusted energy flux estimated soil clay content for the majority (99.5%) of igneous parent materials in California and Oregon (R^2 = 0.67**), the only states with digital geologic data. The model underestimated clay content in steeply sloping Inceptisols and Andisols (0.5% of igneous land area). Results suggest that rates of NPP may be used to estimate soil C for climate regimes with steep environmental gradients. Landscape age and stability components might improve clay prediction in young and erosive landscapes. Modeled energy input provides a tool for estimating pedogenic environments, soil order, and soil properties. Energy input parameters may aid efforts to pre-map broad landscape units for soil survey.**

Current pedogenic modeling strategies vary greatly and include the use of pedotransfer functions, geostatistical estimation of soil properties and stochastic models of soil processes, often combined with the use of geographic information systems (GIS), digital elevation models (DEMs), and soil databases (Hoosbeek et al., 2000). At the core of many of these models remains a dependence on the classic state factor equation first presented by Dokuchaev (1883), and formalized by Jenny (1941).

The emergence of regional, national, and statewide digital data sets of soil properties, climate variables, remotely sensed vegetation data, DEMs, and geologic parent material has allowed quantitative testing of the state factor equation and its ability to predict soil properties from the reasonably well-known relationships between environmental variables and pedogenesis. Zhu et al. (2001) contend that if the relationship between a soil and its environment is known, then soil characteristics can be inferred from landscape properties and environmental conditions. This type of evaluation is the basis for the qualitative segregation of soils on the landscape and soil field mapping (Buol et al., 2003).

Examples of pedogenic modeling using established databases are numerous. Bernoux et al. (2002) provided estimates of soil C stocks based on soil-vegetation associations derived from soil and vegetation databases. Wu et al. (2001) coupled soil survey information with remotely sensed data to identify land use change, land use potential, and best management practices. Klingebiel et al. (1988) demonstrated the efficacy of using DEM data in first order soil mapping and landscape classification. Zhu et al. (2001) combined GIS modeling tools with a soil–land inference model and expert soil scientist knowledge of local landscape relationships to map a landscape soil continuum. These models use a generalized state factor model approach, and demonstrate the potential for landscape unit segregation and state factor modeling using environmental databases and GIS. Our model is also based on the generalized state factor equation; however, we attempt to quantify external energy inputs and soil parent material to predict pedogenic environments and soil properties. Following Runge (1973), our model assumes that soil properties and distinct soil forming environments may be predicted by rates of energy input from precipitation and NPP into the soil system.

It is hypothesized that ecological systems, such as soil systems, tend to self organize to optimize the use of energy flowing into and through the system, with the degree of ordering directly related to the overall energy flow (Morowitz, 1968; Odum, 1983). Energy from solar radiation, in the form of NPP (E_{npp}) and precipitation (E_{ppt}), represent the dominant source of energy input into most soil systems. Open system thermodynamic theory has been used as a means to describe the self organization, entropy minimization, and free energy maximization of natural systems (Morowitz, 1968; Smeck et al., 1983; Addiscott, 1994) and is used as the basis of our

Land, Air, and Water Resources Dep., Univ. of California, One Shields Ave., Davis, CA 95616; C. Rasmussen, present address: Soil, Water, and Environmental Science Dep., Univ. of Arizona, Shantz Bldg. #38, PO Box 210038, Tucson, AZ 85721. This work was funded by USDA Cooperative Agreement No. 68-7482-7-240 and Donald Crosby Fellowship funds awarded to Craig Rasmussen. Received 29 Oct. 2003. *Corresponding author (crasmuss@ag.arizona.edu).

Published in Soil Sci. Soc. Am. J. 69:1266–1274 (2005).
Pedology
doi:10.2136/sssaj2003.0283
© Soil Science Society of America
677 S. Segoe Rd., Madison, WI 53711 USA

Abbreviations: DEM, digital elevation model; E_{in}, total energy input; E_{npp}, energy from net primary production; E_{ppt}, energy from effective precipitation; GIS, geographic information systems; MAAT, mean annual air temperature; MAT, mean air temperature; NPP, net primary production; P_{eff}, effective precipitation; PMI, parent material index; PRISM, parameter-regression independent slope model; STATSGO, state soil geographic database; **, significant in the 0.01 probability level; ***significant at the 0.001 probability level.

Reproduced from Soil Science Society of America Journal. Published by Soil Science Society of America. All copyrights reserved.

14350661, 2005, 4, Downloaded from https://acsess.onlinelibrary.wiley.com/doi/10.2136/sssaj2003.0283 by University Of Arizona Library, Wiley Online Library on [29/12/2025]. See the Terms and Conditions (https://onlinelibrary.wiley.com/terms-and-conditions) on Wiley Online Library for rules of use; OA articles are governed by the applicable Creative Commons License

model hypothesis that soil system properties may be estimated by energy input.

Morowitz (1968) described a generalized system outlining energy flow through ecological systems. The overall system may be divided into two parts, the source–sink system, and the intermediate system. In the case of soils, the source–sink system represents external energy import and export, while the intermediate system is the soil system or pedon (Fig. 1). Pedon processes include ordering functions such as humus accumulation, horizonation, structure development, illuviation–eluviation, and secondary mineral formation, as well as dissipative processes that export energy from the pedon (Smeck et al., 1983; Addiscott, 1994) (Fig. 1). In the case of the soil system, the external environment may be the atmosphere above the soil surface (e.g., the loss of CO_2 to the atmosphere due to humus decomposition processes) or the lower pedon limit, with the loss of solutes to groundwater and stream waters.

The degree of organization within the soil system is directly related to the balance between ordering and dissipative processes and the amount of energy flowing through the soil system, such that greater energy flow will generate greater ordering within the pedon (Smeck et al., 1983). In terms of free energy, the initial condition of the soil system represents a relatively low free energy state (e.g., primary minerals far from equilibrium with surface conditions and an overall large, negative free energy state). The rate of energy flow through the system is equivalent to the potential increase in free energy of the system, such that greater energy flow will equate to a greater increase in the free energy state of the pedon. For example, soils in warm humid climates with a large flow of energy from precipitation, will reach a higher level of organization and free energy state relative to soils in cool arid areas (Smeck et al., 1983). It thus follows that a quantification of the energy input to a soil system should represent the soil forming environment and potentially the developmental state of the soil system.

It has been suggested that soil systems will store energy (e.g., in the form of soil C) in amounts relative to the rate of energy input as a means to sustain the system and catalyze the inflow of additional energy (Anderson, 1995). In soil systems at steady state with current energy input, soil C content should reflect a balance between the rate of NPP and the energy or nutrient demands of the soil system. Likewise, clay production and alteration of parent material will be strongly related to the energy flow through the system that is derived from precipitation and water moving through the soil column (Runge, 1973). Therefore, an assessment of energy input associated with NPP and precipitation should allow for estimation of soil properties, assuming the soil system is at or near steady-state conditions.

Our objectives in this study were to predict pedogenic environments based on energy inputs from NPP and precipitation. As a means to test our estimates of energy input, we compare rates of precipitation-derived energy to field based weathering rates and compare rates of NPP to those estimated for global ecosystems. We further test the hypothesis that rates of energy input may be used to predict soil order, soil C, and clay content. We applied this model at the state and regional scale in California, Oregon, Washington, North Dakota, Texas, Alabama, Pennsylvania, and New Hampshire, thereby covering a wide range of climatic regimes. The main objective of this model is to provide a quantitative framework that may be used to characterize soil forming environments and expected soil properties, independent of soil data.

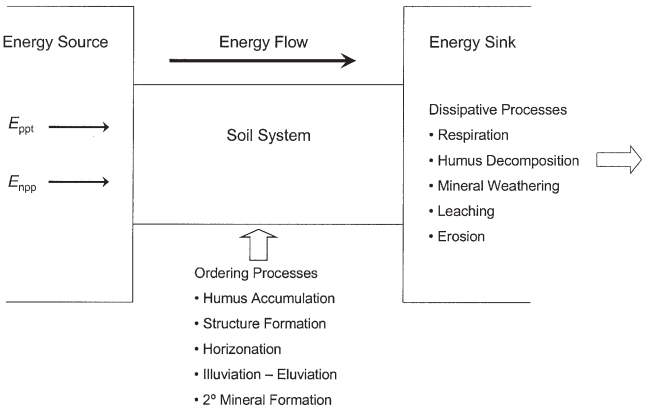

Fig. 1. Schematic representation of energy flow through an open soil system showing the three essential features: an energy source (energy from effective precipitation [E_{ppt}] and energy from net primary production [E_{npp}] both derived from solar radiation), an energy sink, and the soil system through which energy flows. Ordering processes represent entropy minimization within the soil system and dissipative processes represent entropy export from the soil system to the source-sink system (Modified from Morowitz, 1968; Smeck et al., 1983; and Addiscott, 1994).

MODEL DEVELOPMENT

The factorial model of Jenny (1961) was used as a basis for developing our model Eq. [1]

$$S = f(L_o, P_x, t) \quad [1]$$

where S is the soil state, L_o is the initial state of the system, P_x is external flux factors, and t is the age of the system. The initial state includes characteristics of the geologic substrate and topography, while the external flux factors include energy inputs from precipitation and NPP. The specific energy inputs of our model include energy from effective precipitation and energy from NPP. To characterize parent material and initial conditions, we used a weatherability index or PMI based on chemical and physical properties of the parent rock.

While time and landscape age are an integral part of this model, we did not attempt to include time in this modeling exercise because of the difficulty in estimating landscape age at a regional scale. We are using data on a 4 by 4 km basis (see below for dataset description). At this scale, many of the subtleties of landscape age are lost in data aggregation. For example, the Central Valley of California contains soils that range in age from late Holocene to early Pleistocene within a 16-km^2 area. Our model is an attempt to quantify current pedogenic regimes, such that the rate of energy input into the soil system is used to isolate distinct pedogenic environ-

ments. We suggest that for the majority of soils, characterizing current pedogenic regimes will allow for estimation of soil properties and the degree of soil development.

Energy, Net Primary Production, and Parent Material Index Calculations

Energy

Climate is considered one of the most important factors of soil formation (Jenny, 1961). In particular, water availability and temperature act as controls of many soil properties and plant community distribution (Birkeland, 1974; Neilson, 2003). The amount and timing of water flux largely determines the rate and trajectory of soil genesis by facilitating the dissolution and reorganization of the soil mineral assemblage, providing a chemical reactant for hydrolysis reactions, as well as water to drive NPP (Arkley, 1963; Alvarez and Lavado, 1998; Chadwick and Chorover, 2001).

Climate conditions play a significant role in determining solute chemistry and weathering rates, with the temperature of precipitation affecting both thermodynamic and kinetic interactions between minerals and solutions (Birkeland, 1974; White and Blum, 1995). Weathering is related to the amount of water available to move through the soil system, but the efficiency of that water as a solvent, and hence as a weathering agent, increases with an increase in temperature, such that warm waters have a greater ability to weather minerals. The greater weathering potential of warm water will more rapidly move the soil system toward a higher free energy state. Thus, soils systems with a greater flux of warm water through the pedon should correspond to highly weathered, well developed soils.

Our precipitation energy calculation is based on the premise that air temperature at the time of precipitation controls soil temperature and the temperature of soil water and hence, potential rates of mineral weathering. We based our precipitation energy estimation on the amount of precipitation (P_{eff}) greater than or equal to potential evapotranspiration (ET_p), assuming the P_{eff} water is available to flow through the soil system. We calculated P_{eff} on a monthly basis, using monthly precipitation data and ET_p estimated using the Thornthwaite Equation (Thornthwaite, 1948).

We estimated an energy input associated with P_{eff}, by assuming that P_{eff} water was heated from 0°C to the mean air temperature (MAT) for that respective month. The underlying assumption is that soil temperature approaches MAT and that the temperature of water entering the pedon as P_{eff} will be in equilibrium with the soil temperature. The majority of precipitation in middle to high latitudes results from the ice-crystal process, such that the temperature of precipitation is at or below 0°C in the cold (ASCE, 1996), justifying the assumption of heating from 0°C to MAT. Mean air temperature may then be used as a proxy for P_{eff} temperature and provides an approximation of the potential weathering energy (due to temperature) of P_{eff}. We do not estimate kinetic energy of rainfall impact or the kinetic energy of water flow through the soil system. Months where the MAT was less than zero were adjusted to a value of 0°C, to recognize that frozen water produces little energy flow through the soil system.

By assuming a temperature of P_{eff}, we could then calculate the amount of energy in 1 cm^3 packet of water using the specific heat of water. One centimeter of precipitation was assumed to be equivalent to 1 cm^3 of precipitation per cm^2 of soil surface. The amount of energy per soil area could be calculated from the energy associated with each packet of P_{eff} for a given month. These values were then summed for months of P_{eff}, to yield E_{ppt} using Eq. [2]:

$$E_{ppti} = (c)(P_{effi})(MAT_i) \quad [2]$$

where i is month of P_{eff}, c is the specific heat of water (4.18 J g^{-1} °K^{-1}), P_{eff} is the mass of water and MAT represents the change in temperature from 0°C to the MAT.

This energy calculation allows for precipitation and temperature parameters to be combined into one unit describing a portion of the energy flow into the soil system. The integration of climatic energy terms reduces the number of variables used to describe climate influence on soil properties, but still takes into account solar radiation, leaching potential, and weathering potential associated with P_{eff}. This approach does not address those desert systems where, on average, P never exceeds ET_p. These areas were not included in this modeling exercise.

One possible limitation of this type of energy calculation is the estimation of energy associated with precipitation that falls as snow. This calculation assumes that energy associated with snow fall is zero because it has not been heated above freezing and ignores the heat energy needed to melt winter snow pack and the potential energy associated with snow melt. This energy calculation only estimates the energy input of P_{eff} as rain and ignores any temperature change of P_{eff} water once it enters the soil profile. We also do not consider kinetic energy of rainfall impact on the soil surface. Raindrop impact is typically curtailed by the presence of vegetation and may only play a significant role in areas with sparse plant cover (Paton et al., 1995).

Net Primary Production

A biologic energy input was calculated based on NPP determined from an empirical relationship developed by Lieth (1975b) relating mean annual air temperature (MAAT) to annual NPP. We used a modified calculation of NPP based on P_{eff}, working under the assumption that NPP occurs predominantly during months where water is available for plant growth, and that these months correspond to months of P_{eff}. The temperature during these months is critical to controlling NPP. We used the MAT for each month of P_{eff} to calculate NPP (g dry matter m^{-2} yr^{-1}) on a monthly basis using Lieth's equation relating NPP to MAAT (substituting MAT for MAAT). This NPP value was then corrected for the percentage of time that each month occupies during the

Reproduced from Soil Science Society of America Journal. Published by Soil Science Society of America. All copyrights reserved.

14350661, 2005, 4, Downloaded from https://acsess.onlinelibrary.wiley.com/doi/10.2136/sssaj2003.0283 by University Of Arizona Library, Wiley Online Library on [29/12/2025]. See the Terms and Conditions (https://onlinelibrary.wiley.com/terms-and-conditions) on Wiley Online Library for rules of use; OA articles are governed by the applicable Creative Commons License

Reproduced from Soil Science Society of America Journal. Published by Soil Science Society of America. All copyrights reserved.

14350661, 2005, 4, Downloaded from https://acsess.onlinelibrary.wiley.com/doi/10.2136/sssaj2003.0283 by University Of Arizona Library, Wiley Online Library on [29/12/2025]. See the Terms and Conditions (https://onlinelibrary.wiley.com/terms-and-conditions) on Wiley Online Library for rules of use; OA articles are governed by the applicable Creative Commons License

Table 1. Comparison of net primary production (NPP) estimations.

Ecosystem type	NPP†	P_{eff} NPP‡
	g m^{-2} yr^{-1}	
Temperate evergreen forest	600–2500	485
Woodland and shrubland	250–2000	405
Savanna	200–2000	450
Temperate grassland	200–1500	256
Desert and semidesert scrub	10–250	70

† Modified from Lieth (1975b).
‡ Effective precipitation.

year, and these values then summed to obtain an annual value for NPP Eq. [3].

$$NPP_i = \{3000/[1 + e^{(1.315 - 0.119)(MAT_i)}]\} (days_i/365 \text{ d yr}^{-1}) \quad [3]$$

As with E_{ppt}, the P_{eff} method for calculating NPP does not provide NPP estimates for ecosystems where there is no P_{eff} during the year. These areas were excluded for the purposes of this study.

Table 1 compares our NPP values calculated for California biomes to those estimated by Lieth (1975b) for global biomes. The P_{eff} NPP values are on the low end of the range given for global ecosystems. Most likely NPP also occurs in months immediately following the last month of P_{eff}, while stored soil moisture is still available in the soil profile. Adding these months to the estimation may bring the P_{eff} values in line with those estimated for global ecosystems, but for this exercise, these months were not included in the NPP calculation.

The NPP data were converted to energy input (E_{npp}) rates by assigning an average energy value to each gram of dry matter input from NPP (22.2 kJ g dry matter^{-1}) and converted to a rate per area (Lieth, 1975a). Energy values for different litter components range from 17.1 for woodpolyoses to 36.8 for resins and fats with a standard deviation of 6.8. We did not attempt to change the energy value from NPP input for different vegetation and litter types. Values presented in Lieth (1975a) show little variation in the average energy associated with NPP for global biomes (standard deviation of 1.3 kJ g^{-1} NPP).

Parent Material Index

We use a PMI to describe parent material susceptibility to weathering processes. As a first approximation, we chose to focus our investigation on igneous parent materials, because igneous parent materials present a relatively homogenous composition among rock types, as opposed to sedimentary and metamorphic rocks, which may be of mixed origin. Geologic map units were initially segregated into igneous, metamorphic, and sedimentary rock types. Igneous map units were further classified into five igneous rock types: andesite, basalt, gabbro, granite, and rhyolite.

The PMI values are equivalent to weathering indices estimated from catchment scale observations measuring CO_2 consumption by weathering in runoff for monolithic catchments (Table 2) (Drever and Clow, 1995). The weathering indices were normalized to a value of 1.0 for plutonic, namely granite, rock types. The PMI functions as a unitless coefficient characterizing parent material influence on energy transformation in the soil system. PMI, and total energy input rate (E_{in}, kJ m^{-2} yr^{-1}) were combined to estimate clay formation Eq. [4].

Table 2. Parent material index (PMI) values for igneous parent materials†.

Parent material	PMI
Granite	1.0
Gabbro	5.0
Basalt	5.0
Andesite	2.3
Rhyolite	2.3

†PMI (Parent Material Index) taken from Drever and Clow (1995).

$$E_{in} = E_{npp} + E_{pp}$$

$$Clay = (PMI)(E_{in}) \quad [4]$$

Statewide digital geology data was only available for California and Oregon, and therefore are the only states where the PMI was used for clay estimation.

Databases for Model Building

The PRISM database was used to approximate climatic parameters across the continental USA. The PRISM model interpolates climatic data from known points using the assumed relationship between changes in topography and elevation and changes in temperature and precipitation at a scale of 1:250 000 (Daly et al., 1994). The PRISM data allow for estimation of current pedogenic regimes and we assumed the PRISM data represent the average climatic conditions during pedologically significant lengths of time (i.e., we ignore past climate changes). Parent material data for California were extracted from a digitized geology map based on the 1977 geologic map of California from the California Department of Mines and Geology, at a scale of 1:750 000 (Jennings, 1977). Digital geology data were also available for Oregon at a scale of 1:500 000 (Walker and MacLeod, 1991).

Model Testing

We used STATSGO datasets to test estimations of soil order and soil properties made with the model. We specifically avoided using any soil properties in the model development, to keep our estimations independent of the datasets used for testing. Soil C and clay content and soil order for each STATSGO map unit were compared with NPP rate (= C), E_{in} and PMI rate (= clay) and total E_{in} (= order), respectively. Data were aggregated from soil layers to map units, so that values for both organic C and clay content were assigned to each map unit. Organic C and clay contents were calculated on a kilogram per square meter (kg m^{-2}) basis for the entire pedon using bulk density values and corrected for coarse fragment (>2 mm) content (Bliss et al., 1995). STATSGO does not contain data for organic "O" layers. Organic C from the Forest Inventory Analysis (FIA) (USFS-USDA) for O layers was included in pedon C calculated from STATSGO (S.W. Waltman, personal communication, 2001).

We limited the soil orders used for the C and clay

Reproduced from Soil Science Society of America Journal. Published by Soil Science Society of America. All copyrights reserved.

14350661, 2005, 4, Downloaded from https://acsess.onlinelibrary.wiley.com/doi/10.2136/sssaj2003.0283 by University Of Arizona Library, Wiley Online Library on [29/12/2025]. See the Terms and Conditions (https://onlinelibrary.wiley.com/terms-and-conditions) on Wiley Online Library for rules of use; OA articles are governed by the applicable Creative Commons License

content modeling exercise to Entisols, Mollisols, Inceptisols, Alfisols, Andisols, Spodosols, and Ultisols. Oxisols and Gelisols represent a very small portion of the land area of the states we analyzed, so were not included in model validation. Areas of rock outcrop and urban land were also excluded. Any map units containing a Histosol component were not included because of the lack of mineral soil material and extreme C accumulation that is mostly a function of poor drainage and slow decomposition, rather than high levels of NPP. Vertisols were excluded because of the high clay content inherent in the fine-textured alluvial or eolian deposits that typically form the parent material for this soil order. Aridisols were not included in the validation of C and clay predictions. Despite the fact that they are largely defined by their climatic regime, they may include soils with a wide range of soil properties due to large variations in landscape age and external sources of parent material, such as eolian deposition. However, we did include Aridisols in the characterization of the total energy flux in each soil order.

Rates of NPP and E_{in} were compared with soil C and clay pools calculated from STATSGO data. We assumed that greater NPP and E_{in} input rates correspond to greater soil C and clay content, respectively. Input rate values were compared directly to soil values on a pixel-by-pixel basis. The data were also evaluated using a natural break classification scheme to more easily evaluate trends in soil variables with input rates. Input rate data were classified into 15 classes as described by Jenks (1963, 1977). This classification scheme minimizes the variance around the mean of each class and maximizes the variance between classes. We chose 15 classes so each class had a minimum of 10 pixels (most classes contained hundreds or thousands of pixels). Soil data were then averaged within each class and plotted versus the input class to identify trends of increasing C or clay content with increasing rates of input.

Total E_{in} was characterized by soil order for each state. Map units were assigned to a soil order if >40% of the components in that map unit were of one soil order. All other map units were not used in this exercise because of the high variability of soil orders within those map units. Total E_{in} and the percentage of E_{in} accounted for by E_{npp} and E_{ppt} were averaged for each soil order to determine if soil orders are represented by differences in total energy input and the relative proportion of each energy type.

Data Analysis and Manipulation

All data manipulation and analysis was conducted using ArcGIS 8.3 (ESRI, Inc, Redlands, CA). Data layers were reprojected relative to the PRISM data, using a Geographic Coordinate system and WGS 1972 datum. Polygonal data layers were converted to raster images with a cell size of 4 by 4 km to match that of the original PRISM data layers. Raster calculations were performed using the Raster Calculator and Grid Editor module of ArcGIS 8.3. Statistical analysis was done using SPSS (SPSS, Inc, Chicago, IL) and data plotting was performed in SigmaPlot (SPSS, Inc., Chicago, IL). Energy variables by soil order were analyzed using an ANOVA with Tamhane post hoc test for pairwise comparison of means at the 95% confidence interval. The non-parametric Tamhane test was used because energy variables could not be transformed to meet assumptions of homogeneity of variance. Linear regression analysis between input classes and soil pools was performed by comparing Jenk's classified input variables to STATSGO soil data using a weighted linear regression, where the number of pixels in each Jenk's class weighted the regression analysis. Reported regression coefficients are based on the classified data.

RESULTS AND DISCUSSION

Energy Input, Mean Annual Precipitation, and Mean Annual Air Temperature

Figure 2 depicts E_{in} versus MAAT and MAP for the continental USA. The pattern of E_{in} corresponds with the idealized relationship between clay percent and mean annual moisture and temperature proposed by Jenny (1941) for soils derived from granite and gneiss. The pattern of E_{in} also corresponds to the model White and Blum (1995) fit to MAAT, MAP, and stream Si flux data from granitoid watersheds across the USA. A similar pattern of E_{in} to that of watershed Si flux suggests a relationship between our estimated energy input and actual rates of weathering measured in natural soil systems. We compared E_{in} directly with Si flux data from the sites examined by White and Blum (1995) and found a significant linear relationship between the two variables (Fig. 3), suggesting that E_{in} effectively describes potential weathering rates in these granitoid watersheds.

Soil Orders and Energy Input

Smeck et al. (1983) suggest the energy state of a soil system may be related to soil order, for example, Enti-

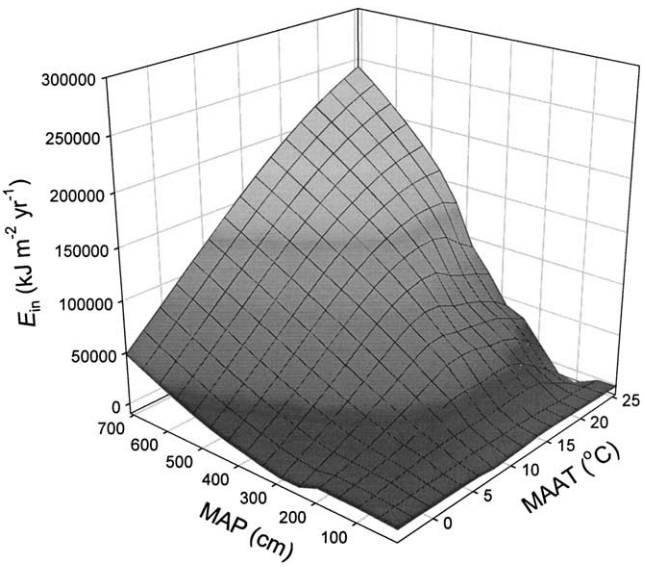

Fig. 2. Modeled total energy input (E_{in}) versus mean annual precipitation (MAP) and mean annual air temperature (MAAT) for the continental USA.

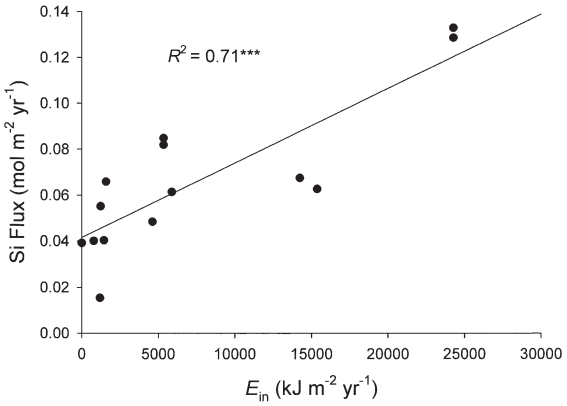

Fig. 3. Silica flux from granitoid watershed across the continental USA versus total energy input (E_{in}) estimated from regional climate datasets. Silica flux data is from White and Blum (1995) and references therein.

sols grade to Inceptisols to Alfisols to Ultisols and finally to Oxisols with greater total energy input. With this concept in mind, we quantified the annual rate of E_{in} and the distribution of E_{npp} and E_{ppt} by soil order for all of the states to characterize differences in energy input and soil forming processes between soil orders. It is important to highlight that E_{in} is a rate based on current climate conditions and is independent of elapsed time; landscape age and past climate change were not considered in this analysis for reasons mentioned above.

There were clear and significant separations of E_{in} by soil order (Fig. 4). Aridisols stand alone as having the lowest E_{in}, suggesting that under current climatic conditions, Aridisols have low climatic and biologic fluxes. Entisols and Mollisols group together with similar E_{in} rates, both slightly greater than that of the Aridisols. Andisols and Alfisols show progressively higher rates of E_{in}. Following these orders, E_{in} increases significantly, grading from Inceptisols to Spodosols and finally to Ultisols, which have the greatest E_{in} of the orders characterized.

The calculated E_{in} by soil order fits the conceptual model of soil formation and soil properties reflecting the energy input into that system (Smeck et al., 1983). Inceptisols, however, stand out as having a high E_{in} relative to Alfisols and Andisols, and appear to occur in soil forming environments more like those of Spodosols

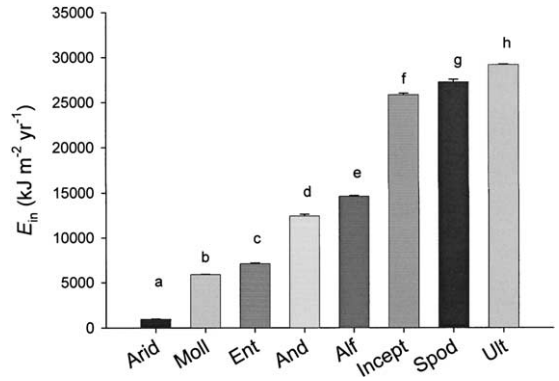

Fig. 4. Average total energy input (E_{in}) by soil order, data aggregated for all states. Different lowercase letters signify significantly different values for mean E_{in}.

Table 3. Average slope for soil orders†.

Soil order	Slope %‡
Andisol	26 (2.1) a
Inceptisol	26 (1.2) a
Spodosol	26 (3.4) ab
Entisol	15 (1.1) bc
Mollisol	12 (0.5) cd
Alfisol	10 (0.7) de
Ultisol	10 (0.5) e
Aridisol	9 (1.9) cde

† Average of map unit slope from STATSGO.
‡ Values in parentheses are standard errors of the mean. Pairwise comparison done with Tamhane post-hoc test (95% confidence interval). Slopes followed by the same lowercase letter are not significantly different.

and Ultisols than of Alfisols or Andisols. An analysis of the average STATSGO map unit slope by soil order indicates that Inceptisols have a significantly greater slope than all of the other soil orders except for Andisols and Spodosols (Table 3). This suggests that erosion, slope stability, and lateral movement of fine fraction material (Paton et al., 1995) may limit the development of Inceptisols, and prevent them from developing the argillic or kandic horizons of Alfisols or Ultisols. The high slope for Andisols and Spodosols can be explained by the fact that most of the Andisols and Spodosols in this study are located in mountainous regions of coastal Oregon and Washington formed from young volcanic ash deposits.

We also calculated the relative energy input of E_{ppt} and E_{npp} as a percentage of E_{in} (Fig. 5). Energy distribution may serve as a proxy for the dominant soil forming process in each soil order. Aridisols have the lowest E_{in}, but this flux is dominated by E_{npp}, suggesting that these soils are dominated by biologic processes. This analysis does not consider chemical reactions driven by evaporative processes or eolian deposition. Mollisols, Andisols, and Entisols are all dominated by E_{npp}, again suggesting a dominance of biology driven processes in these soils.

Alfisol energy distribution shows a shift toward greater influence of E_{ppt}. Inceptisols, Spodosols, and Ultisols grade toward a dominance of E_{ppt}, suggesting similar soil forming processes dominating these soil orders. Interestingly, Inceptisols have a much greater E_{in} and slope than Alfisols, suggesting that on stable landscapes,

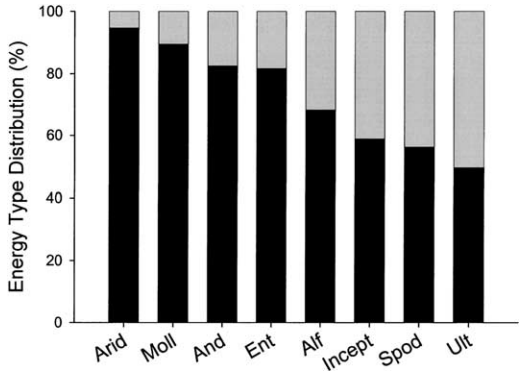

Fig. 5. Distribution of energy from net primary production (E_{npp}) and energy from effective precipitation (E_{ppt}) as a percent of total energy input (E_{in}) by soil order, data aggregated for all states. The E_{npp} (black) represents energy input from net primary production and E_{ppt} (gray) represents energy input from precipitation.

Reproduced from Soil Science Society of America Journal. Published by Soil Science Society of America. All copyrights reserved.

14350661, 2005, 4, Downloaded from https://acsess.onlinelibrary.wiley.com/doi/10.2136/sssaj2003.0283 by University Of Arizona Library, Wiley Online Library on [29/12/2025]. See the Terms and Conditions (https://onlinelibrary.wiley.com/terms-and-conditions) on Wiley Online Library for rules of use; OA articles are governed by the applicable Creative Commons License

Reproduced from Soil Science Society of America Journal. Published by Soil Science Society of America. All copyrights reserved.

14350661, 2005, 4, Downloaded from https://acsess.onlinelibrary.wiley.com/doi/10.2136/sssaj2003.0283 by University Of Arizona Library, Wiley Online Library on [29/12/2025]. See the Terms and Conditions (https://onlinelibrary.wiley.com/terms-and-conditions) on Wiley Online Library for rules of use; OA articles are governed by the applicable Creative Commons License

Inceptisols may evolve toward Alfisols or Ultisols with the formation of diagnostic subsurface argillic or kandic horizons. The majority of Inceptisols may represent systems where soil properties are far from steady state with respect to input fluxes because of erosion processes or landscape age. Ultisols show the greatest input from E_{ppt}, suggesting a significant role of energy input from precipitation, and a dominance of chemical weathering, translocation and leaching processes in these soil orders.

Soil Property Estimation

Carbon Content

As an initial comparison of climate parameters and soil C, we compared the number of months of P_{eff} to regional soil C data aggregated from each state (R^2 = 0.67***). The significant relationship between the number of months of P_{eff} and soil C suggests a seasonal control of NPP based on the months where excess water is available for plant production. However, this empirical relationship does not allow for prediction of rates of NPP and E_{npp}. Because of this, we assumed the temperature of these months was critical to NPP and used this data to estimate rates of NPP as described above.

We aggregated NPP and soil C data from each state to test the model on a national scale. At this scale we found a poor fit (R^2 = 0.03) between modeled rate of NPP and soil C pools. We also separated states into regional areas; (west [California, Oregon, Washington], central [Texas, North Dakota], and east [Alabama, Pennsylvania, New Hampshire]) and compared modeled NPP data to soil C in each region. The ability to predict soil C content varied by region, with a significant positive correlation found in the west (R^2 = 0.86***) and no significant trends found in the central and east regions (R^2 = 0.08 and R^2 = 0.05, respectively). The west region stands apart from the central and east in that it is characterized by steep environmental gradients, with large differences between minimum and maximum values for MAAT, MAP, annual ETp, and NPP (Table 4). In the west, it appears that the steep climatic gradients associated with orographic rainout in the Sierra Nevada and Cascade ranges may override local landform controls of soil C, allowing for estimation of soil C with rates of NPP calculated from climate data.

Another possible explanation for the lack of fit in the central and east regions is that our model of NPP may only be appropriate for the western region, dominated by strong seasonal variation in precipitation. Net primary production models designed specifically for the central and east regions may provide a more accurate estimate of soil C stocks. It is also possible that soil C content is not at steady state with current climate conditions and NPP inputs in the central and east regions, suggesting landscape age and past NPP rates may be necessary for estimation of soil C directly from NPP.

Table 4. Regional Environmental Gradients†.

Region‡	MAP	MAAT	ET_p	P_{eff} NPP
	cm	°C	cm	g m^{-2} yr^{-1}
West	5–646	−4–24	32–816	70–1200
Middle	22–149	2–23	51–469	30–660
East	267–788	2–20	45–243	255–1140

† Range of values (minimum–maximum).
‡ West (California, Oregon, Washington); Middle (Texas, North Dakota); and East (Alabama, Pennsylvania, New Hampshire).

Clay Content on Igneous Parent Materials

We focused our clay estimation on areas of California and Oregon underlain by igneous parent materials. Figure 6 shows estimation of clay content by E_{in} classes without the inclusion of the PMI variable. There is a clear break in the data between E_{in} Classes 10 and 11. The majority of the igneous land area is contained in Classes 1 through 10, which represent nearly 99% of modeled land area. Classes 11 through 15 represent approximately 1% of the igneous land area. These soils with high energy input have considerably less clay than predicted with E_{in} and are located in the Coast Ranges and mid-elevation Sierra Nevada and Cascades. The soils in this high E_{in} group are mostly Inceptisols and Andisols, with a smaller number of Alfisols and Ultisols in the northern Sierra Nevada of California in Class 11. The majority of these areas have steeply sloping landscapes (calculated as an average of STATSGO map unit slopes), suggesting landscape stability may be limiting clay accumulation in these sites. The small land area of underpredicted clay, the distinct geographic distribution of these soils, and unique soil order and slope properties suggest these are unique soil forming environments.

When we included the PMI variable in our clay estimation for the same igneous areas, the data again group into two sets, although there is an improvement in the overall regression coefficient (R^2 = 0.48** vs. R^2 = 0.67***). Over 99.5% of the pixels now fall into the first group (1–11) of E_{in} classes (as compared with 99% without PMI), while roughly 0.5% of the pixels fall into the higher E_{in} class (12–15) grouping. Thus, the incorporation of PMI transferred over 50% of the land area formerly in the higher E_{in} group into the lower E_{in}

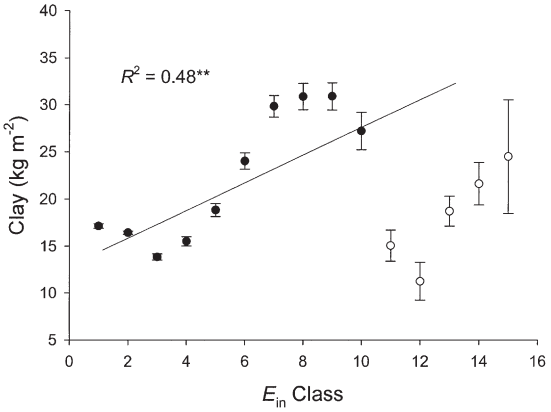

Fig. 6. The total energy input (E_{in}) Jenk's classes and clay content for igneous subset of California and Oregon. Filled circles represent 99% of the igneous land area in California and Oregon. Open circles represent 1% of igneous land area and are located in the Coast Ranges and mid-elevation areas of the Sierra Nevada and Cascade ranges.

Reproduced from Soil Science Society of America Journal. Published by Soil Science Society of America. All copyrights reserved.

14350661, 2005, 4, Downloaded from https://acsess.onlinelibrary.wiley.com/doi/10.2136/sssaj2003.0283 by University Of Arizona Library, Wiley Online Library on [29/12/2025]. See the Terms and Conditions (https://onlinelibrary.wiley.com/terms-and-conditions) on Wiley Online Library for rules of use; OA articles are governed by the applicable Creative Commons License

group. The higher E_{in} group again corresponds to Coast Range and mid-elevation Sierra Nevada and Cascade ranges and the majority are steeply sloping Inceptisols and Andisols. The high E_{in}, low clay content Inceptisols and Andisols may represent either highly erosive landscapes or landscapes that have received recent ash deposits. Either of these factors would generate young geomorphic surfaces. We did not include time or landscape age in this model exercise, so we are unable to predict clay in these systems that have high energy input but occur on unstable landscapes.

A limitation to the PMI concerns the scale difference between the geology and soil data (1:750 000 and 1:500 000 vs. 1:250 000), which most likely introduces errors in assigning soil pixels a PMI. The PMI parameter may be optimized at finer scales (<1:250 000) with more detailed information of parent material composition.

SUMMARY

This model was built on the premise that the state of a soil system is a function of energy input into the soil system. We inferred energy input from climatic data to estimate soil forming environments and soil properties. Our model is derived from the state factor approach and may be used to represent pedogenic regimes and possibly as a predictor of soil order and soil properties by quantifying energy inputs and the initial system conditions. Total energy input and the relative proportion of energy input from NPP and precipitation by soil order fit with our conceptual model of soils as open systems whose organization and state is a function of the energy flowing through them.

At the regional STATSGO scale, modeled NPP rates provided reasonable estimations of organic C content in western states, but failed to predict soil C in central and eastern states. Clay content was reasonably predicted on igneous parent materials in California and Oregon from energy inputs estimated solely from climate data, with the exception of a very small portion (1%) of the landscape dominated by high E_{in} Inceptisols and Andisols with low clay content. The addition of PMI values improved the estimation of clay content by reducing the land area (i.e., to about 0.5% of the total) where clay content was over predicted. The current modeling framework focuses on climate flux in the form of precipitation and NPP and our results show that this approach allows for separation of pedogenic environments and soil orders at the regional scale.

This model may be improved and modified to operate at finer scales, such as the county scale (1:24 000), with the incorporation of landform indices derived from fine-scale DEM data, site specific parent material indices, and remotely sensed vegetation data. These data sources could allow for incorporation of landscape stability features, vegetative cover and type, and specific indices relating parent material composition to weatherability. The incorporation of landscape age in particular, would allow for further testing of the hypothesis that soil properties and pedogenic regimes may be represented by these energy input variables. This approach, developed independent of soil data, may be useful for soil survey premapping and separation of the landscape into pedogenic environments.

ACKNOWLEDGMENTS

We thank Sharon Waltman, USDA-NRCS, National Soil Survey Center for providing national soil C data. We also thank Donald G. McGahan and anonymous reviewers for their insightful comments and discussion.

REFERENCES

Addiscott. T.M. 1994. Simulation, Prediction, Foretelling or Prophecy? Some thoughts on pedogenetic modeling. p. 1–17. *In* R.B. Bryant and R.W. Arnold (ed.) Quantitative modeling of soil forming processes. SSSA Spec. Pub. 39. SSSA Soil Sci., Madison, WI.

Alvarez, R., and R.S. Lavado. 1998. Climate, organic matter and clay content relationships in the Pampa and Chaco soils, Argentina. Geoderma 83:127–141.

Anderson, D.W. 1995. Decomposition of organic matter and carbon emissions from soils. p. 165–175. *In* R. Lal et al.(ed.) Soils and global change. Lewis Publishers, Boca Raton, FL.

ASCE. 1996. Hydrology handbook. 2nd ed. ASCE, New York.

Arkley, R.J. 1963. Calculation of carbonate and water movement in soil from climate data. Soil Sci. 96:239–248.

Bernoux, M., M.C.S. Carvalho, B. Volkoff, and C.C. Cerri. 2002. Brazil's soil carbon stocks. Soil Sci. Soc. Am. J. 66:888–896.

Birkeland, P.W. 1974. Pedology, weathering, and geomorphological research. Oxford University Press, London.

Bliss, N.B., S.W. Waltman, and G.W. Peterson. 1995. Preparing a soil carbon inventory for the United States using geographic information systems. p. 275–295. *In* R. Lal et al. (ed.) Soils and global change. Lewis Publishers, Boca Raton, FL.

Buol, S.W., R.J. Southard, R.C. Graham, and P.A. McDaniel. 2003. Soil genesis and classification 5th ed. Iowa State Press, Ames, IA.

Chadwick, O.A., and J. Chorover. 2001. The chemistry of pedogenic thresholds. Geoderma 100:321–353.

Daly, C., R.P. Neilson, and D.L. Philips. 1994. A statistical-topographic model for mapping climatological precipitation over mountainous terrain. J. Appl. Meteorol. 33:140–158.

Dokuchaev, V.V. 1883. Russian chernozems (Russkii chernozem). Israel Prog. Sci. Trans., Jerusalem, 1967. Transl. from Russian by N. Kraner. Available from U.S. Dep. of Commerce, Springfield, VA.

Drever, J.I. and D.W, Clow. 1995. Weathering rates in catchments. p. 463–481. *In* A.F. White and S.L. Brantley (ed.) Chemical weathering rates of silicate minerals. Reviews in Mineralogy 31. Mineralogical Society of America. BookCrafters, Inc., Chelsea, MI.

Jenks, G.F. 1963. Generalization in statistical mapping. Ann. Assoc. Am. Geographers. 53:15–26.

Jenks, G.F. 1977. Optimal data classification for chloropleth maps. Cartography Program 01. Department of Geography, University of Kansas, Lawrence, KS.

Jennings, C.W. 1977. Geologic map of California, scale 1:750,000. Division of Mines and Geology, California Dep. of Conservation. Sacramento.

Jenny, H. 1941. Factors of soil formation. A system of quantitative pedology. McGraw-Hill, New York.

Jenny, H. 1961. Derivation of state factor equations of soils and ecosystems. Soil Sci. Soc. Am. Proc. 25:385–388.

Hoosbeek, M.R., R.G. Amundson, and R.B. Bryant. 2000. Pedological modeling. p. E-77–E-111. *In* M.E. Sumner (ed.) Handbook of soil science. CRC Press, Boca Raton, FL.

Klingebiel, A.A., E.H. Horvath, W.U. Reybold, D.G. Moore, E.A. Fosnight, and T.R. Loveland. 1988. A guide for the use of digital elevation model data for making soil surveys. Open File Report No. 88–102. U.S. Gov. Print. Office, Washington, DC.

Lieth, H. 1975a. Measurement of caloric values. p. 119–129. *In* H. Lieth and R.H. Whittaker (ed.) Primary productivity of the biosphere. Springer-Verlag, New York.

Lieth, H. 1975b. Primary production of the major vegetation units of the world. p. 203–215. *In* H. Lieth and R.H. Whittaker (ed.) Primary productivity of the biosphere. Springer-Verlag, New York.

Morowitz, H.J. 1968. Energy flow in biology. Ox Bow Press, Woodbridge, CT.
Neilson, R.P. 2003. The importance of precipitation seasonality in controlling vegetation distribution. p. 47–71. *In* J.F. Weltzin and G.R. McPerson (ed.) Changing precipitation regimes and terrestrial ecosystems. A North American perspective. University of Arizona Press, Tucson.
Odum, H.T. 1983. Systems ecology: An introduction. John Wiley & Sons, New York.
Paton, T.R., G.S. Humphreys, and P.B. Mitchell. 1995. Soils a new global view. UCL Press, London.
Runge, E.C.A. 1973. Soil development sequences and energy models. Soil Sci. 115:183–193.
Smeck, N.E., E.C.A. Runge, and E.E. Mackintosh. 1983. Dynamics and genetic modeling of soil systems. p. 51–81. *In* L.P. Wilding et al. (ed.) Pedogenesis and soil taxonomy. Elsevier, New York.
Thornthwaite, C.W. 1948. An approach toward a rational classification of climate. Geograph. Rev. 38:55–94.
Walker, G.W., and N.S. MacLeod. 1991. Geologic map of Oregon, scale 1:500,000. U.S. Geological Survey. Portland, OR.
White, A.F., and A.E. Blum. 1995. Effects of climate on chemical weathering in watersheds. Geochim. Cosmochim. Acta 59:1729–1747.
Wu, J., M.D. Ransom, G.J. Kluitenberg, M.D. Nellis, and H.L. Seyler. 2001. Land-use management using a soil survey geographic database for Finney County, Kansas. Soil Sci. Soc. Am. J. 65:169–177.
Zhu, A.X., B. Hudson, J. Burt, K. Lubich, and D. Simonson. 2001. Soil mapping using GIS, expert knowledge, and fuzzy logic. Soil Sci. Soc. Am. J. 65:1463–1472.

Reproduced from Soil Science Society of America Journal. Published by Soil Science Society of America. All copyrights reserved.

14350661, 2005, 4, Downloaded from https://acsess.onlinelibrary.wiley.com/doi/10.2136/sssaj2003.0283 by University Of Arizona Library, Wiley Online Library on [29/12/2025]. See the Terms and Conditions (https://onlinelibrary.wiley.com/terms-and-conditions) on Wiley Online Library for rules of use; OA articles are governed by the applicable Creative Commons License